EXECUTIVE SUMMARY OF THE THESIS

# Estimate and Uncertainty Assessment of Onshore Geological $CO_2$ Storage Capacity with Application to Potential Reservoirs across China

TESI MAGISTRALE IN ENERGY ENGINEERING – INGEGNERIA ENERGETICA
OIL&GAS PRODUCTION

**AUTHOR: RAFI KHATTAR**

**ADVISOR: PROF. ALBERTO GUADAGNINI**

**CO-ADVISORS: PROF. MARTIN J. BLUNT, PROF. FABIO INZOLI, DR. EHSAN RANAEE**

**ACADEMIC YEAR: 2020-2021**

## 1. Introduction

Increasing rates of greenhouse gas emissions as a result of human activity have led to a lifeline problem that requires joint global effort. By the end of current century, the world is on track for 2.4 °C of warming.

In 2020, the world's total carbon dioxide ($CO_2$) emissions reached 31.5 Gt, representing an increase of almost 50% since 2000. Of this, the share of China is the biggest, being the world's largest energy consumer and carbon emitter (IEA, 2021). For this reason, the role of China is vital to meet the emission reductions targets to limit the global temperature rise to 1.5 °C.

Peaking the emissions requires progress in energy efficiency, renewables and reducing fossil fuels use, and while the first two are progressively developing, the latter may be the hardest due to the still high dependency of many countries on traditional energy. Consequently, Carbon Capture and Storage is considered a crucial strategy for meeting $CO_2$ emission reduction targets (Leung et al., 2014), with the $CO_2$ injected in a supercritical state.

The most suitable formations are deep saline aquifers and depleted oil and gas reservoirs, being able to offer the largest capacity (Energy Technology Perspectives, 2020). Storage capacity is the main parameter for assessing the quantity of $CO_2$ that can be held by the formation (Bachu et al., 2007). For its estimation, we rely on pressure build-up techniques, which provide conservative results.

We assess the capacity of the 10 most suitable basins in China. Cumulative storage capacity over such 10 basins can reasonably represent the global capacity of onshore geological $CO_2$ storage in China. Moreover, we perform an uncertainty assessment and Global Sensitivity Analysis (GSA) to address the solidity of the evaluated storage capacity and understand the most influential model input parameters.

# 2. Energy Sector and $CO_2$ Emission in China

## 2.1 Energy Sector

China is heavily dependent on fossil fuels, with coal (the most carbon intensive) accounting for 60 % of its energy needs (CEC, 2021). Table 1 provides the amount of emissions per sector and the number of units, in China. Clearly, the energy sector is the leading emitters among the industrial activities. Thus, CCS is expected to (potentially) be able to provide great supports in reducing emissions effects.

| Sources | $CO_2$ emissions (Mt/y) | Number of units |
|---|---|---|
| Power and heat generation | 5000 | 450 |
| Chemicals | 600 | 60 |
| Iron and steel | 1390 | 650 |
| Cement | 1210 | 800 |
| Fuel refining | 270 | 120 |
| **Total** | **8470** | **2080** |

Table 1: Evaluation of $CO_2$ emissions in China divided by source types and the related number of units (IEA, 2020).

Recently, IEA (2021) reported an Energy Sector Roadmap to Carbon Neutrality in China and proposed different scenarios which evaluate the share of CCS necessary to meet emissions targets. In the Announced Pledges Scenario (APS), it estimates a total of 2.6 Gt of $CO_2$ to be stored in 2060, in China. We assume a worst-case scenario when the required injection is constant and fixed at this value and not increasing in the years as proposed in the APS. In this work, we propose 30 years target (of 80 Gt in total) to meet the requirements of the APS.

## 2.2 CCS in China

The development of CCS in China is still on the early stages. Currently, 21 pilot (mostly injecting $CO_2$ for enhanced oil recovery, EOR, purposes), demonstration or commercial project are in operation.

CCS is set to be an indispensable technology for carbon neutrality in China, as a result of the large role of coal in its energy mix. CCS retrofits are the only way to avoid the early disruption of recently built plants running on coal and still meeting the emissions targets.

Figure 1 is a map of the main $CO_2$ emitter points in China, together with some potential geological storage formations and pipelines which are already present in the territory. The combination of the emission points with the suitable basins is fundamental for its economic feasibility and success.

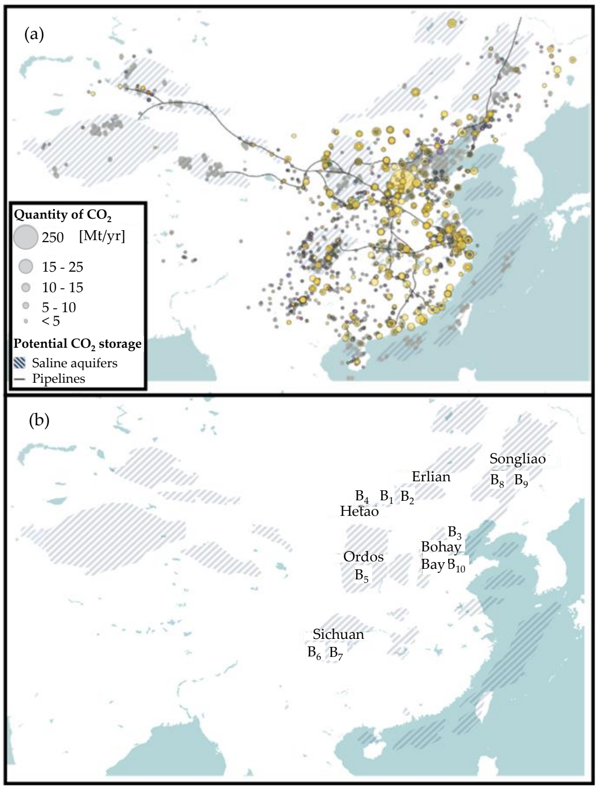


Figure 1: Map of (a) $CO_2$ sources and (b) potential geological storage basins (B1-B10) selected for the analysis of storage $CO_2$ capacity in China (IEA, 2021).

# 3. Material and Methods

We rely on the methodology developed by De Simone and Krevor (2021). This technique embeds constraints associated with the increase of reservoir pore pressure due to injection of $CO_2$ in the presence of resident brine so that an excessive pressure build-up must be limited to avoid reactivation of faults, failure of caprock, and/or possible leakage (Bachu, 2008).

The tool used to estimate the largest viable injection rate and reservoir storage capacity is the open-source software CO2BLOCK (De Simone and Krevor, 2021). It builds different scenarios in terms of number of injection wells and inter-well spacing through which it selects the one with maximum storage capacity. Karvounis and Blunt (2021) has been recently used this approach to assess storage capacity in the North Sea.

For simplicity purposes, and to be consistent with the aim of performing a global storage capacity assessment of the kind we consider, we assume: (i) the reservoir to be conceptualized as a homogeneous system and (ii) number of $n$ vertical injection wells to be placed across the domain, with uniform spacing and operating at the same (constant) volumetric injection rate.

### 3.1.1 Pressure build-up due to $CO_2$ injection

The pressure buildup following $CO_2$ injection from a single well into a homogeneous reservoir with open boundaries and under the assumption of no pre-existing fractures and negligible trapping can be evaluated according to Nordbotten et al. (2005). Additionally, the action of multiple wells can then be expressed through superposition and, assuming no interference in $CO_2$ plumes associated with each of the injection wells, the overpressure at a location $\boldsymbol{x}_i$ of well $i$ can be evaluated as (De Simone and Krevor, 2021):

$$\Delta p_{sup}(\boldsymbol{x}_i, t) = \frac{Q\mu_w}{2\pi kH}\left[\frac{\mu_c}{\mu_w}\ln\left(\frac{\psi}{r_0}\right) + \ln\left(\frac{R}{\psi}\right) + \sum_{j=2}^{n}\ln\left(\frac{R}{d_{ij}}\right)\right] \quad (1)$$

where $\Delta p(r, t)$ is overpressure at time $t$ and radial distance $r$ from the injection well operating at volumetric flow rate $Q$; $k$, $\phi$, and $H$ are absolute permeability, porosity, and average thickness of the reservoir, respectively; $\mu_w$ and $\mu_c$ are brine and $CO_2$ dynamic viscosity, respectively; $\psi$ represents the radius of a fictitious equivalent advancing vertical sharp interface between the injected plume and the resident fluid, which can be expressed as $\psi = \exp(\omega)\xi$ (where $\omega = \frac{\mu_c+\mu_w}{\mu_c-\mu_w}\ln\sqrt{\frac{\mu_c}{\mu_w}} - 1$; $\xi = \sqrt{\frac{Qt}{\pi\phi H}}$); $r_0$ is the well radius, $d_{ij}$ is the distance between wells at (vector) locations $\boldsymbol{x}_i$ and $\boldsymbol{x}_j$ ($\boldsymbol{x}_i$ denoting the vector of spatial coordinates of well $i$) and $R$ corresponds to the well radius of influence.

### 3.1.2 Constraints to pressure build-up

Pressure build-up must be kept below a critical value corresponding to the largest pressure, $\Delta p_M$, sustainable by the system. Jaeger et al. (2009) show that formation failure may occur in either a tensile or a shear mode. Accordingly, the largest sustainable overpressure ($\Delta p_M$) is then evaluated as the lowest between tensile- and shear-related failure pressure values.

### 3.1.3 Constraints to the maximum flowrate

Starting from Equation (1), we evaluate the overpressure, $\Delta p_r$, due to a preliminary value of $CO_2$ injection rate ($Q_r$) at a well, which is taken as reference and is maintained constant across a given temporal window. We build several scenarios considering different numbers of wells and inter-well spacing for a given total injection rate into the reservoir unit.

Once the maximum sustainable overpressure $\Delta p_M$ is assessed and the overpressure, $\Delta p_r$, associated with the reference injection rate, $Q_r$, is evaluated, one can then evaluate the largest sustainable injection flowrate ($Q_M$) into each well. In this context, De Simone and Krevor (2021) suggest the following formulation to evaluate the maximum flow rate, $Q_M$, given the response (in terms of overpressure) for a reference scenario:

$$Q_M(t) = -\frac{Q_r\widetilde{\Delta p_M}}{W\left(-\widetilde{\Delta p_M}e^{-\widetilde{\Delta p_r(t)}}\right)} \quad (2)$$

where $W$ denotes the Lambert function (e.g., Corless et al., 1996) for $-\widetilde{\Delta p_M}e^{-\widetilde{\Delta p_r(t)}} < 0$; $\widetilde{\Delta p_M} = \frac{\Delta p_M}{bQ_r}$ and $\widetilde{\Delta p_r} = \frac{\Delta p_r}{bQ_r}$ with $b = \frac{\mu_w-\mu_c}{4\pi\kappa H\rho_c}$, $\rho_c$ being $CO_2$ density. It is recalled that both the reference and the maximum sustainable flow rates correspond to mass injection into each well.

Calculations of the storage capacity for a given time $t$, $V_M = ntQ_M$, is then straightforward.

Finally, we calculate values of $V_M$ for different scenarios encompassing various numbers of wells and inter-well distances to select the maximum possible overall capacity of the reservoir.

## 3.2 Global Sensitivity Analysis and Uncertainty Assessment

Quantifying the way uncertainties associated with the parameters embedded in the model propagate to its outputs can help identifying the most influential model parameters with respect to the target model response.

We consider parameters $A$, $H$, $\phi$, $k$, $c$ included in the mathematical formulations presented in Section 3.1 as uncertain. For the purpose of our application, we neglect uncertainties linked to $CO_2$/brine properties (e.g., density and viscosity). We introduce vector $\boldsymbol{\theta}$ whose entries $\theta_i$ ($i$ = 1, …, $N_P$) correspond to the values of these $N_P$ = 5 uncertain model parameters.

We rely on modern Global Sensitivity Analysis (GSA) approaches and focus on the maximum $CO_2$ storage capacity of a target reservoir, $Y = V_{CO_2}$, and quantify the contribution of each uncertain model parameter to its uncertainty.

To do so, we take advantage of the recent moment-based global sensitivity metrics introduced by Dell'Oca et al. (2017), denoted as $AMA$ indices.

$AMAE_{\theta_i}^{Y}$, $AMAV_{\theta_i}^{Y}$ and $AMA\gamma_{\theta_i}^{Y}$ represent the sensitivity indices associated with the mean, variance, and skewness of $Y(\boldsymbol{\theta})$, respectively ($E(\bullet)$ denotes expected value, $V(\bullet)$ denotes variance and $\gamma(\bullet)$ being skewness). They quantify the expected change of mean, variance, and skewness of $Y$ due to variations of $\theta_i$, respectively. The combined use of these indices enables one to perform a comprehensive GSA of the target model response, $Y(\boldsymbol{\theta})$, quantifying the impact of each entry of $\boldsymbol{\theta}$ on the variability of $Y$.

These indices allow for a comprehensive description of how the structure of the *pdf* of $Y$ is affected by variations of uncertain model parameters.

# 4. Results

## 4.1 Characteristics of the Analyzed Basins

Basins introduced in Figure 1 are analyzed (preliminarily) here for the assessment of suitability for $CO_2$ storage. We follow Wei et al. (2012) GIS-based framework of analysis, which reports that the basins in Figure 1b are potentially suitable for $CO_2$ storage. The objectives considered are 4: (*i*) storage capacity and injectivity; (*ii*) risk minimization and storage security; (*iii*) environmental restrictions, and (*iv*) economic considerations.

Authors show that 90% of $CO_2$ sources are (within a maximum of) 160 km from one of selected $CO_2$ storage reservoir; this allows to justify the total costs and needed technology for geological storage of $CO_2$, on commercial scale in China (Dahowski et al., 2009).

## 4.2 Uncertainty assessment

Following the definition of a list of uncertain model parameters $\theta_i$ (with i= {1, …,5}). We refer to the information reported in the literature (Zeng et al., 2013; Diao et al., 2017; Fan et al., 2014; Wang et al., 2018; Jin et al., 2017) and assign relatively broad ranges of support to the values of $\theta_i$ uncertain variables.

We assume values of the uncertain parameter being uniformly distributed. For $\theta_1 = H$, we decide a ± 50 % range of support around the mean values reported in the literature; uncertainty in $\theta_2 = A$ of ± 20%; the variation of $\theta_3 = log_{10}$(k) is in the range of ± 1. Porosity is correlated to permeability as $\phi = a\,log_{10}$(k), such that the porosity and permeability of the sampling simulation parameters matches. We impose a support range of ± 0.03 to the values of a $\theta_4 = a$. Therefore, for every value of permeability generated a corresponding value of porosity is quasi-randomly created. Accordingly, uncertainty in values of $\phi$ arises from the product of uncertainties in values of $\theta_3$ and $\theta_4$. Sample values of $\theta_5 = log_2$(c) are uniformly generated in a support range of ± 1 around mean value reported in the literature.

Values of each $\theta_i$ parameter is then reflected into the values of the mathematical model (see Section 3.1) parameter of $A, H, \phi, k$ and $c$ as represented in Figure 2. As clearly illustrated, the sample pdfs of the values of mathematical model parameter do not necessarily follow uniform distributions, Figure 2 reports its distributions.

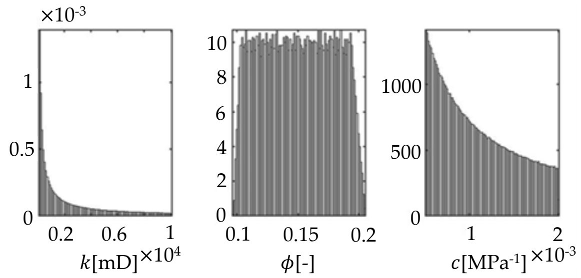


Figure 2: Distribution of sample realizations of uncertain parameters $(\phi, k, c)$. Sample realizations $A$, and $H$ (not shown here) are uniformly distributed

An ensemble of realizations is generated by sampling from supporting range of uncertain parameters and the storage capacity of each $j$ reservoirs, $V(B_j)$, is evaluated. The total number of realizations generated is $10^4$. Total capacity, $V(B_{tot})$, is evaluated for the sum of realization values calculated over 10 studied basins.

Figure 3 and Figure 4 provide the stability of mean, variance, skewness, and standard deviation (over mean) of the values of storage capacity with respect to the number of realizations. All graphs illustrate stability of MC simulation results (in terms of $CO_2$ storage capacity) is achieved after almost 5000 realizations.

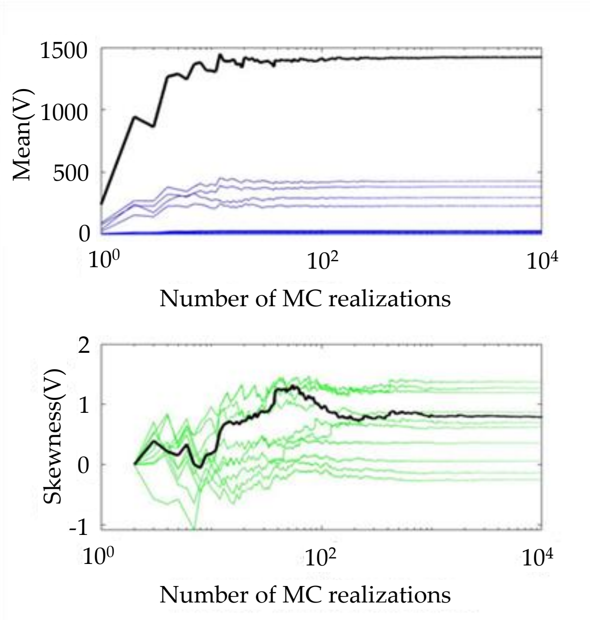


Figure 3: Stability of Mean and Skewness of the storage capacity of the studied basins of our study

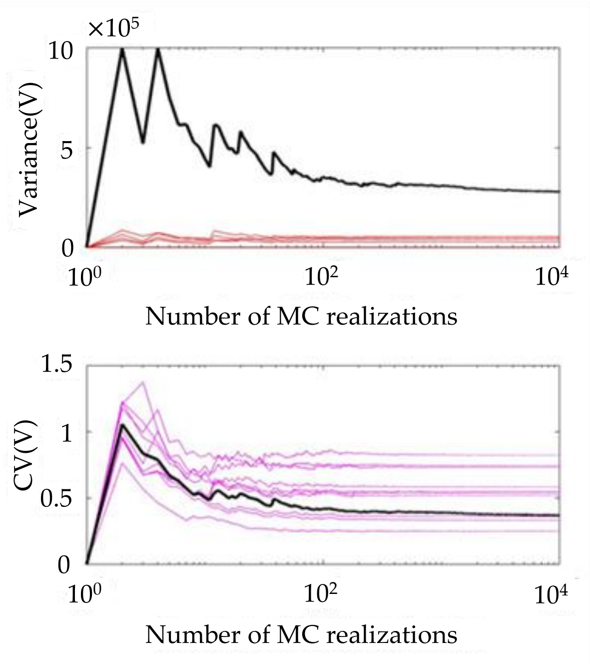


Figure 4: Stability of Variance and Standard Deviation (over Mean) of the storage capacity of the studied basins of our study.

We quantify the degree of similarity between two different pdfs of the storage capacity increasing number of realizations in terms of the changes in Kullback - Leibler divergence, KLD (Kullback and Leibler, 1951). Small values of the KLD confirm that the MC simulations can reliably reproduce the distribution of storage capacity. Figure 5 shows that pdfs converge when we consider 6000 or more realizations.

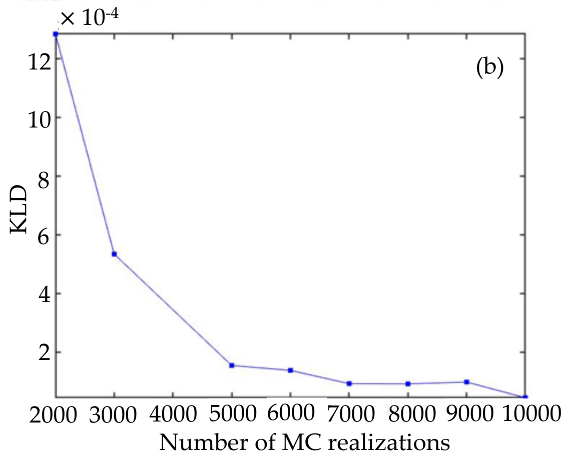


Figure 5: Values of KLD reported for sampled pdf of $V(B_{tot})$ values generated for selected subsequent sets

## 4.3 Sensitivity Analysis

We quantify the sensitivity of the simulation model outputs (i.e., $Y = V(B_i)$) with respect to the variations in the values of uncertain parameters, $\theta_i$, referring to the approach introduced in Section 3.2.

We obtain that uncertainty in rock/fluid properties, as well as reservoir size all influence estimations of $CO_2$ storage capacity of the relatively large basins, with small values of permeability; otherwise, for small basins with intermediate values of permeability, rock properties (i.e., $\phi$ and $k$) appear to be the most important parameters. Fluid properties and height of the reservoir are mainly influence simulation results of very large basins with relatively high values of porosity/permeability.

## 4.4 Estimation of Storage Capacity

Simulation results illustrate that sample pdfs of the potential storage capacity are different for the different basins. More precisely, we can see how sampled pdf of $V(B_j)$ for large basins with high permeability (i.e., $B_1$-$B_2$-$B_{10}$) produce more normal kind distributions. Small basins of $B_3$, $B_5$ (even with high permeability) show some skewness to the high values of $V(B_j)$. The combination of large basins and small permeability ($B_4$-$B_6$-$B_7$) produces some skewness to the small values. The sampled pdfs of the very large basins ($B_8$-$B_9$) show skewness to high values.

Left skewed distributions can be related to the constraint imposed to the simulations by the minimum interwell distance (i.e., 3 km), which for small reservoir becomes restrictive accumulating most of the sustainable scenarios to the left of the mode. Otherwise, a right skewed distribution is due to the engineering constraints assumed (i.e., $Q_s$ = 5 Mt/y per well) which limit the storage capacity achievable by a given number of wells.

To summarize simulation results, Figure 6 reports the sample pdf of $V(B_{tot})$ in conjunction with the boxplot reporting the median, located around 1400 Gt (red line), and the range of third quantiles (25% to 75%) in 1100-1700 Gt. We have some outliers in the tail to the high values confirming that distribution of the $V(B_{tot})$ values do not follow a normal distribution. As we reported in section 2.2, $CO_2$ emissions to be abated in China for the next 30 years, are expected to be 80 Gt (according to APS). This can be so far behind the supporting range of the third quintile of $V(B_{tot})$, as reported in Figure 6. Accordingly, the storage capacity of China seems to be robust and able to meet the needs of most of the $CO_2$ emissions around the territory, with multiple possibilities to pair emission sources to the storage sites.

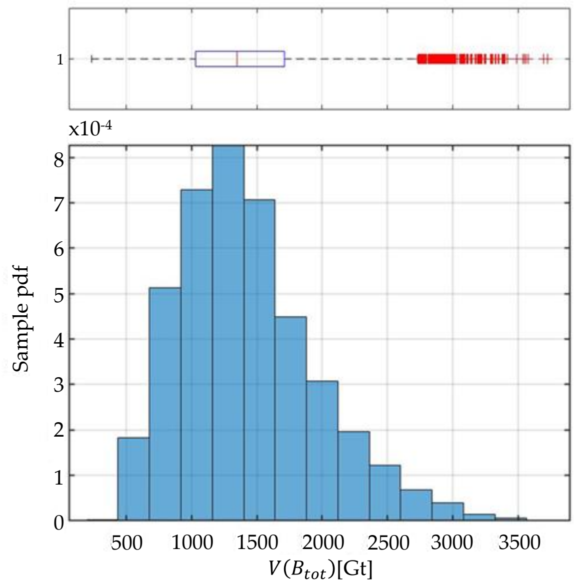


Figure 6: Sample pdf of total $CO_2$ storage capacity, $V(B_{tot})$, in 10 selected basins of China.

## 5. Conclusions

Carbon capture and storage is fundamental to reach net-zero purposes. This study aimed to estimate the total geological storage capacity of some main basins in China. A total of 10 reservoirs are analyzed preliminarily and selected following suitable economic, environmental, and geophysical characteristics. We performed simulation of the onshore $CO_2$ storage capacity in China.

Our study confirms an average of 1400 Gt (within a support range of [1100-1700] Gt) of $CO_2$ that can be stored in geological formations during 30 years in China. Present work confirms that CCS technology can fully sustain the required needs of $CO_2$ capture in China.

The uncertainty assessment and sensitivity analysis provided an important insight into the most influencing parameters and the behavioral anomalies of the reservoirs due to their characteristics.

Results provided in this work can be used as a first step for further decision making, detailed investigations, and developments of CCS projects.

Performed uncertainty assessment offers important insights on the most influencing parameters and on the behavioral anomalies of the reservoirs due to their characteristics. This information can be used as a guideline for investigative and decision-making purposes. Furthermore, a source-sink matching (e.g., Wei et al., 2013) analysis, can assure an economical and feasible implementation of the technology, which may encounter substantial costs in case of long-range $CO_2$ transport needs.

## 6. References

Bachu, S., Bonijoly, D., Bradshaw, J., Burruss, R., Holloway, S., Christensen, N. P., & Mathiassen, O. M. (2007). CO2 storage capacity estimation: Methodology and gaps. *International Journal of Greenhouse Gas Control*, *1*(4). https://doi.org/10.1016/S1750-5836(07)00086-2

Celia, M. A. (2017). Geological storage of captured carbon dioxide as a large-scale carbon mitigation option. In *Water Resources Research* (Vol. 53, Issue 5). https://doi.org/10.1002/2017WR020841

Corless, R., Gonnet, G., Hare, D., Jeffrey, D., & Knuth, D. (1996). On the Lambert W Function. *Advances in Computational Mathematics*, *5*, 329–359. https://doi.org/10.1007/BF02124750

Dahowski, R. T., Li, X., & Dooley, J. J. (2009). *Regional Opportunities for Carbon Dioxide Capture and Storage in China The effective pressure law for permeability of clay-rich sandstones View project Demonstration of Key Technologies for Clean and Efficient Utilization of Low-Rank Coal, R&D of CO2 Geological Storage View project*. https://www.researchgate.net/publication/259674766

de Simone, S., Krevor, S. (2021). A tool for first order estimates and optimisation of dynamic storage resource capacity in saline aquifers. *International Journal of Greenhouse Gas Control*, *106*. https://doi.org/10.1016/j.ijggc.2021.103258

Dell'Oca, A., Riva, M., & Guadagnini, A. (2017). Moment-based metrics for global sensitivity analysis of hydrological systems. *Hydrology and Earth System Sciences*, *21*(12). https://doi.org/10.5194/hess-21-6219-2017

Diao, Y., Zhu, G., Cao, H., Zhang, C., Li, X., & Jin, X. (2017). Mesoscale assessment of CO2 storage potential and geological suitability for target area selection in the Sichuan Basin. *Geofluids*, *2017*. https://doi.org/10.1155/2017/9587872

Fan, J., Guo, J., Zhang, S., & Ji, X. (2014). $CO_2$ Geological Storage Suitability Assessment of Sichuan Basin. *Journal of Applied Mathematics and Physics*, *02*(11). https://doi.org/10.4236/jamp.2014.211115

IEA (2020), Energy Technology Perspectives 2020, IEA, https://www.iea.org/reports/energy-technology-perspectives-2020

IEA (2021), An Energy Sector Roadmap to Carbon Neutrality in China. CC BY-NC 3.0 IGO

IEA (2021), Coal 2021 - Analysis and forecast to 2024. In International Energy Agency.

IEA (2021), Global Energy Review 2021, IEA, Paris https://www.iea.org/reports/global-energy-review-2021

Jaeger, J. C., Cook, N. G. W., & Zimmerman,

Jin, C., Liu, L., Li, Y., & Zeng, R. (2017). Capacity assessment of CO2 storage in deep saline aquifers by mineral trapping and the implications for Songliao Basin, Northeast China. *Energy Science and Engineering*, *5*(2). https://doi.org/10.1002/ese3.151

Karvounis, P., Blunt, M. J. (2021). Assessment of CO2 geological storage capacity of saline aquifers under the North Sea. *International Journal of Greenhouse Gas Control*, *111*. https://doi.org/10.1016/j.ijggc.2021.103463

Kullback, S., & Leibler, R. A. (1951). On Information and Sufficiency. *The Annals of Mathematical Statistics*, *22*(1). https://doi.org/10.1214/aoms/1177729694

Leung, D. Y. C., Caramanna, G., & Maroto-Valer, M. M. (2014). An overview of current status of carbon dioxide capture and storage technologies. In *Renewable and Sustainable Energy*

*Reviews* (Vol. 39). https://doi.org/10.1016/j.rser.2014.07.093

Nordbotten, J. M., Celia, M. A., & Bachu, S. (2005). Injection and storage of CO2 in deep saline aquifers: Analytical solution for CO2 plume evolution during injection. *Transport in Porous Media*, *58*(3). https://doi.org/10.1007/s11242-004-0670-9

R. (2009). Fundamentals of Rock Mechanics, 4th Edition. In 4th Edition.

Wang, S., Vincent, C. J., Zeng, R., & Stephenson, M. H. (2018). Geological suitability and capacity of CO2 storage in the Jiyang Depression, East China. *Greenhouse Gases: Science and Technology*, *8*(4). https://doi.org/10.1002/ghg.1782

Wei, N., Li, X., Wang, Y., Dahowski, R. T., Davidson, C. L., & Bromhal, G. S. (2013). A preliminary sub-basin scale evaluation framework of site suitability for onshore aquifer-based CO2 storage in China. *International Journal of Greenhouse Gas Control*, *12*. https://doi.org/10.1016/j.ijggc.2012.10.012

Zeng, R., Vincent, C. J., Tian, X., Stephenson, M. H., Wang, S., & Xu, W. (2013). New potential carbon emission reduction enterprises in China: Deep geological storage of CO2 emitted through industrial usage of coal in China. *Greenhouse Gases: Science and Technology*, *3*(2). https://doi.org/10.1002/ghg.1314

## 7. Acknowledgements

First and foremost, I am extremely grateful to my supervisors Professor Alberto Guadagnini, Professor Martin Julian Blunt and Professor Fabio Inzoli for supporting me in this final step of my academic career and sharing the passion for knowledge, progress, and sustainability.

I would like to thank Dr. Ehsan Ranaee for being my guide and my motivator and teaching me confidence and optimism. It was a big pleasure working with you.

I wish to show my appreciation to Eng. Luigi Urbinati, Dr. Panagiotis Karvounis, Dr. Silvia De Simone for their technical support.

I also thank Regione Lombardia, Politecnico di Milano, Servizio Residenze and DSU scolarship office for the financial and technical aid given, which made all this possible or at least way easier.

I would also like to acknowledge the principal Daniela Verdi, my colleagues, my 140 students and the Pandini high school itself for the amazing experience of teaching and for giving a new color to my life.

I am grateful to my friends and mentors who supported me and advised me consistently, from near or far.

Thank you to Paola for being such a kind, sweet and patient partner and providing me with unfailing support and continuous encouragement throughout my years of study.

A special thanks to my family for never doubting me. Thank you for making me a responsible and independent person and giving me the opportunity to pursue my career.